JMEPEG (2005) 14:343-350
DOI: 10.1361/10599490523986

1059-9495/$19.00

Negative Effects of Reactive Sputtering in an Industrial Plasma Nitriding

E. Roliński, J. Arner, and G. Sharp

(Submitted June 11, 2004; in revised form March 18, 2005)

Plasma nitriding of a 3%Cr-Mo-V gear, a 310 SS PM slot, a 304 SS flat-disk, and an Inconel 718 fillet were performed to demonstrate the effects of reactive sputtering on case-depth uniformity. It was shown that the geometry of the sample in combination with the wrong processing pressure may have a negative influence on the distribution of the vapor-deposited phase, leading to the uneven concentration of a deposit from plasma on the nitrided surface. The presence of this deposit coincides with the disturbance of case-depth uniformity.

Keywords deposit from plasma, nitrided layer uniformity, plasma nitriding, sputtering

1. Introduction

The role of sputtering in ion nitriding has been studied by many researchers (Ref 1-13). Generally, sputtering is considered to be a positive phenomenon, which enhances surface activation processes, especially important in the nitriding of stainless steels (Ref 14). Stainless steels are considered to be difficult to nitride due to various problems with surface activation, which affects the ability of the steel to nitride or to form a uniform layer. The most common problems causing nonuniform case formation or inconsistent results in the nitriding of stainless steels are attributed to imperfections in the finishing techniques of the product as well as to a presence of the native oxides on the surface (Ref 15, 16). Improper, too fast, or too aggressive machining may leave a smeared or a burned layer on the surface, which prohibits the complete chemisorption of the active nitrogen species. This layer will not be removed easily by even the most aggressive sputter cleaning of the surface. Instead, it should to be removed by sand blasting, shot peening, or improved machining.

On the other hand, the native oxides always present on the stainless steel surface may be quickly destroyed by the plasma under typical ramping conditions. Usually, preheating to the nitriding temperature is performed at a low gas pressure at which the highest-energy ions possible in the system are created. Certain standards and studies recommend special surface preparation techniques for stainless steels and limit the time period between cleaning and nitriding to 2 h (Ref 16). This requirement does not seem to be fully justified in plasma nitriding. For example, 304 stainless steel samples, which were stored in the shop environment for five years without any surface preparation, were treated, and the same results were obtained as with freshly vapor degreased and sandblasted samples. The problems with successful plasma nitriding of stainless steels are often associated with passivation or mechanical imperfections on the surface. Providing that the surface preparation was performed correctly, the remaining factor of vacuum imperfections, the presence of oxygen, can play a negative and significant role in prohibiting layer formation in the stainless steel. On the other hand, plasma nitriding of low-alloy and plain carbon steels is not affected by the addition of up to 3% of oxygen to the nitriding atmosphere (Ref 17). Although the above problems do exist in daily industrial processing, they are very often not properly identified or are confused with the real cause. In larger production loads, another phenomenon plays an important role in prohibiting case formation in both stainless steel and non-stainless steel parts: the interference of native and foreign atoms transferred to the nitrided surface by the plasma. There are two main sources of these atoms: sputtering from the load; and sputtering from the fixturing. The work of Tibbets (Ref 18) as well as Michel et al. (Ref 10) showed that the active nitrogen species that formed in the glow discharge plasma play an essential role in the case formation, and therefore, reactive sputtering is not the phenomenon responsible for nitrogen transfer to the cathode workpiece.

Nevertheless, sputtering cannot be neglected as a cause of the mass exchange in plasma nitriding. The rate of material removal from the cathode due to sputtering is an order of magnitude less than 1 μm/h (Ref 13). The sputtered atoms react with the gas molecules and are redeposited on the cathode (Ref 1-3, 6, 7). Their origin varies with some coming from the workload itself, and some coming from the fixturing, masking, and racking. On the way to the cathode, all of these metallic atoms react not only with nitrogen, but also preferably with oxygen atoms, which are always present in industrial systems and may form an oxide containing, a usually dark deposit on the surface. This type of deposit can affect the formation of the nitrided layer and impair its uniformity in stainless steels and also in low-alloy steels (Ref 7). The distribution of the redeposited atoms is very likely to be dependent on the configuration of the electric field around the part. This is often described in the literature as "the workpiece geometry" (Ref 19, 20). Nayal et al. (Ref 19) found that the nitrogen concentration at the cutting edge of a drill during plasma nitriding was systematically higher than that a round sample with the same diameter, due to an increased surface area and the current density at

E. Roliński and **G. Sharp,** Advanced Heat Treat Corp. Waterloo, IA 50703; and **J. Arner,** Struers Inc. Westlake, OH 44145. Contact e-mail: doctorglow@sbcglobal.net.

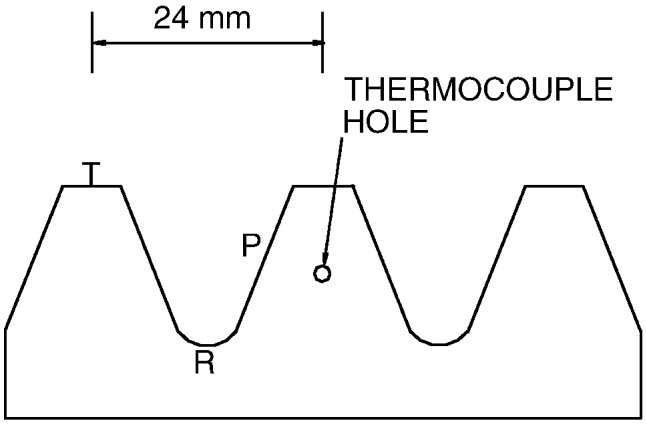

Fig. 1 Gear sample. The width of the sample is 50 mm. R, root; P, pitch; T, tip

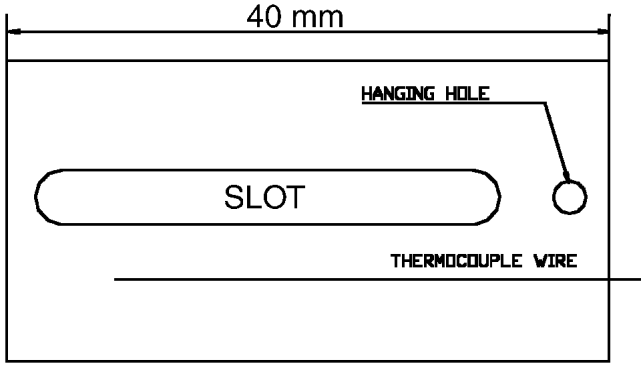

Fig. 2 Slot sample. The thickness of the sample was 5 mm.

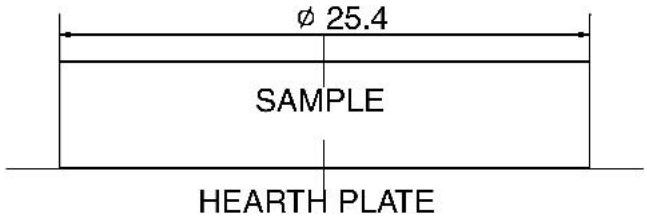

Fig. 3 Disc sample run directly on the hearth plate

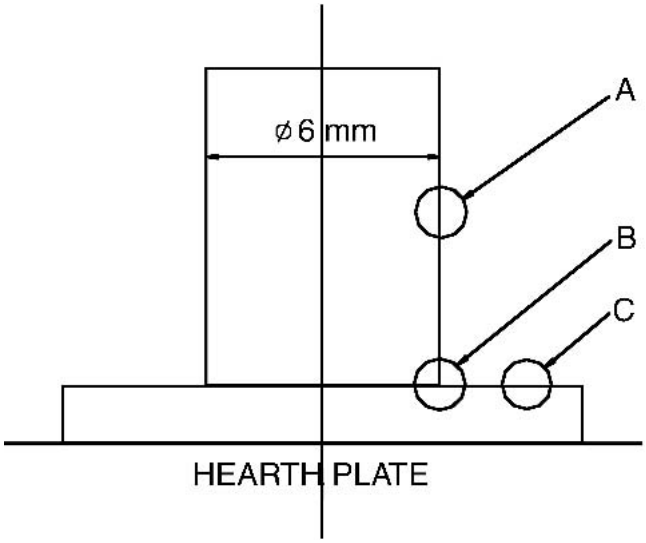

Fig. 4 Fillet sample

Table 1 Samples and processing parameters

Sample type	Material	Temperature, °C	Gas composition, (N_2 + H_2)%	Time, h	Pressure, mbar
Gear	3%Cr-Mo-V	538	30 + 70	354	3.20
Slot	P/M 310 SS	580	50 + 50	15	5.30
Flat disc	304 SS	580	50 + 50	15	3.00
Fillet	Inconel 718	580	70 + 30	70	8.00

the cutting edge. Alves et al. (Ref 20) concluded that at relatively high pressures there is a discontinuity in the observable glow sheath around cylinder-type samples, leading to a temperature gradient in the load that, consequently, affects the case uniformity. The disorder in the electric field configuration around complex geometrical parts, like gears, causes nonuniform deposition and redeposition of the reactive sputtering products, which may cause nonuniform nitriding. Even a simple interference in the plasma configuration, caused by the shape of a 3.2Cr-0.5Mo steel disc sample, resulted in differences in surface structure (Ref 9) and uneven layer formation in the case of austenitic stainless steel samples (Ref 18, 21). Preliminary observations show that there are two negative aspects of the reactive sputtering from plasma. First, when the deposit is formed on the nitrided surface during ramping, and below the nitriding temperature it may completely block access of the active nitrogen species to the surface, prohibiting nitriding from occurring. Second, when the deposit is formed slowly at the nitriding temperature, its presence affects nitriding kinetics. In both situations, the redistribution of the deposit is related to sample geometry. The purpose of this research is to show the most common situations in which reactive sputtering has a negative effect in the plasma-nitriding process.

2. Experimental

2.1 Materials

To illustrate the effect of mass redeposition due to the configuration of the load on the uniformity of the nitrided case, experiments were carried out on a gear, a narrow slot, a fillet, and a round flat disc, as shown in Table 1.

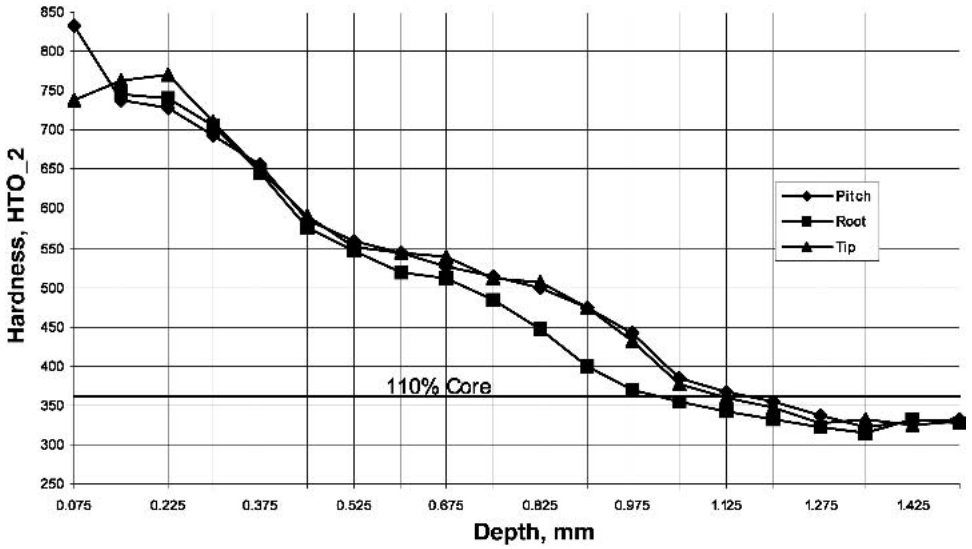

Fig. 5 Microhardness of the 3%Cr-Mo-V steel gear sample after nitriding at 538 °C for 354 h at 3.2 mbar in a mixture of 30% N_2 and 70% H_2. The horizontal line in the graph represents 110% of the core hardness, which was the criterion used for total case definition.

The gear samples were made from 3%Cr-Mo-V steel (Ref 13). The remaining samples were made from commercially available stainless steels and Inconel 718. The slot samples were made from commercial P/M 310 SS, and the flat samples were made from 304 SS. The configurations of the samples in the experiments are shown in Fig. 1 to 4.

2.2 Processing

The nitriding was carried out in the industrial-type, cold-wall, pulse-powered unit with a 0.6 × 0.6 × 0.75 m working space. The temperature of the samples was controlled by thermocouples either directly inserted into the samples, as shown in Fig. 1 and 2, or inserted into the cathode hearth plate. Special attention was paid to the temperature measurements of the gear sample, which was additionally verified with an infrared thermometer (Ref 22). It was found that the temperature difference between the gear root and the gear flank was about 8 °C with the root running cooler. The slot sample was suspended from the fixture, allowing free plasma access to the slot from all directions. The 25.4 mm diameter, 6 mm thick disc sample was located directly on the hearth plate. All of the fixturing elements used in the experiments, as well as the cathodic hearth plate, were made of low-carbon steel and were nitrided previously during production cycles. The flow rate of the fresh gas was about 200 L/h. The amount of flow of the gas through leaks was about 5×10^{-2} mbar-L/s. According to the work of Reinhold et al. (Ref 23), the partial pressure of oxygen should be lower than approximately 5×10^{-3} bar if the nitriding of stainless steels is performed in 100% nitrogen. However, it was also expected that the presence of a sufficient amount of hydrogen in the nitriding atmosphere would lower its oxidizing potential to the level required for the successful nitriding of stainless steels (Ref 23, 24). Even so, it was obvious that the cleanliness of the system was lacking and that under these industrial conditions the nitriding of the stainless steel samples may be impaired (Ref 23).

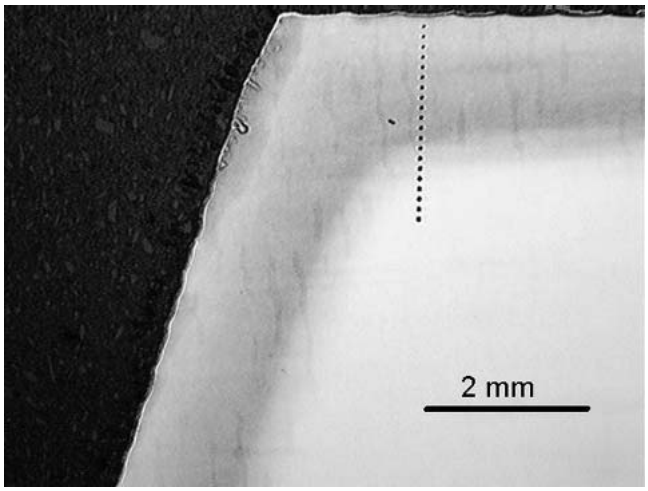

Fig. 6 Photomicrograph of the tip area of the 3%Cr-Mo-V steel gear sample after nitriding at 538 °C for 354 h at 3.2 mbar in a mixture of 30% nitrogen and 70% hydrogen, etched with 2% nital

2.3 Characterization

Metallographic characterization was performed at Struers Center, Inc. (Westlake, OH), using an MEF4M Leica microscope equipped with HV-D25 Hitachi (Tokyo, Japan) camera.

3. Results and Discussion

3.1 3%Cr-Mo-V Gear

The thickness of the nitrided layer in the gear sample was not uniform, as can be seen from the microhardness profiles in Fig. 5 and the photomicrographs in Fig. 6 to 8. The total case depth in the root area, which was determined from the microhardness profile, was approximately 1.00 mm. The layers produced in the pitch and the tip were deeper and had approximately the same thickness at ~1.125 mm. The compound zone in the corner of the tip appeared to be a very compact layer with some porosity near the surface (Fig. 9). The compound zone in

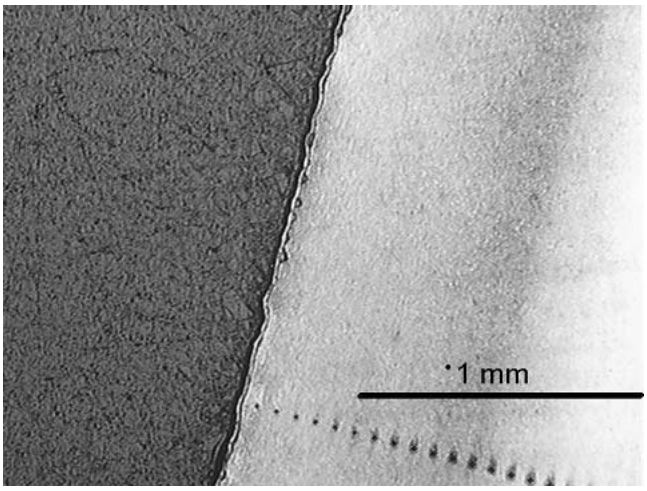

Fig. 7 Photomicrograph of the flank area of the 3%Cr-Mo-V steel gear sample near the pitch diameter after nitriding at 538 °C for 354 h at 3.2 mbar in a mixture of 30% nitrogen and 70% hydrogen, etched with 2% nital

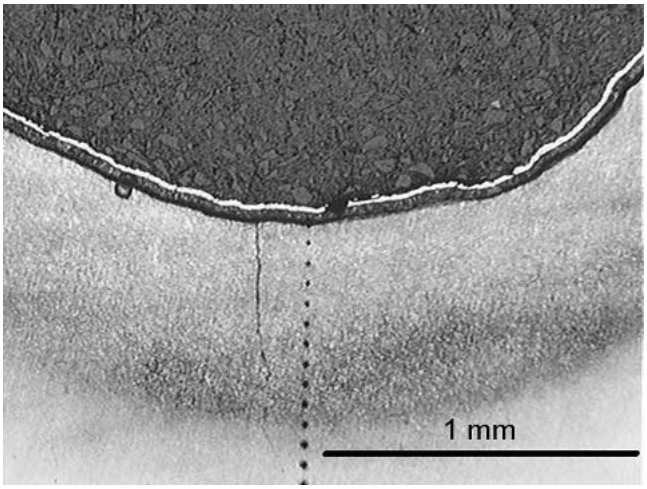

Fig. 8 Photomicrograph of the root area of the 3%Cr-Mo-V steel gear sample after nitriding at 538 °C for 354 h at 3.2 mbar in a mixture of 30% nitrogen and 70% hydrogen, etched with 2% nital. Note the severe porosity near the surface area and a crack approximately parallel to the microhardness indentations.

the pitch was similar, but thinner (Fig. 10). The compound zone in the root area had a different microstructure, a compact portion near the surface and a very porous, easily etched zone underneath (Fig. 8 and 11). At the same time, the compound zone in the root area was much thicker, ~60 μm, and very brittle (Fig. 11). Case depth can be predicted, based on previous work on the same steel (Ref 25), by using the following empirical equation:

$$h = \frac{1}{\left(-4.44 + \frac{82.29}{\sqrt{T}} + \frac{10.46}{\ln t}\right)}$$

where h is the total case depth (in millimeters), T is the temperature (in °C), and t is the time (in hours).

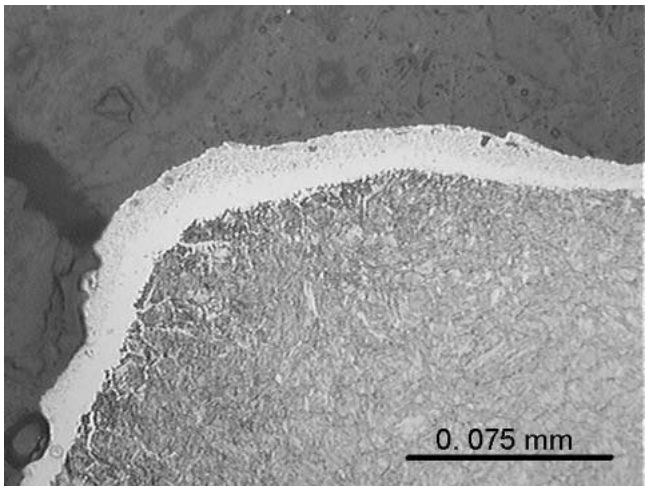

Fig. 9 Photomicrograph of the tip area showing a magnified corner of the 3%Cr-Mo-V steel gear sample after nitriding at 538 °C for 354 h at 3.2 mbar in a mixture of 30% nitrogen and 70% hydrogen, etched with 2% nital. Note the compact form of the compound zone with minor porosity near the surface.

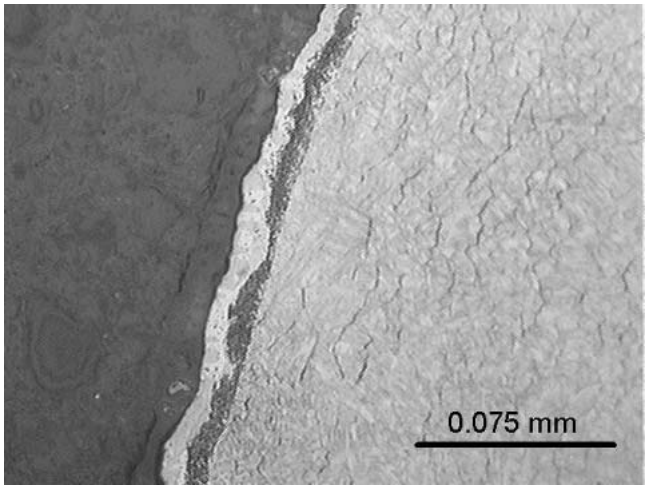

Fig. 10 Photomicrograph of the pitch diameter area of the 3%Cr-Mo-V steel gear sample after nitriding at 538 °C for 354 h at 3.2 mbar in a mixture of 30% nitrogen and 70% hydrogen, etched with 2% nital

The case depth calculated from the equation at 538 °C and the 354 h nitriding time is 1.125 mm, and at 530 °C it is about 1.092 mm. To get the case depth of ~1.00 mm in 354 h, the nitriding temperature would have to be at about 506 °C. The difference in the case-depth thickness between the root and the pitch of the gear sample cannot be explained then by the 8 °C temperature variation. The same applies to the compound zone. The actual compound zone thickness of ~15 μm in the pitch area is in a very good agreement with the value of 12 to 14 μm predicted for 538 °C (Ref 13). Although the exact prediction for compound zone thickness for 530 °C is not available, there is no reason to believe that the lower temperature would not produce a thinner layer. However, the compound zone thickness in the root area is substantially thicker than in any areas of the tooth. The experiments with the gear samples were repeated several times with similar results. The case depth in the root area was always thinner, and the compound zone was thicker in

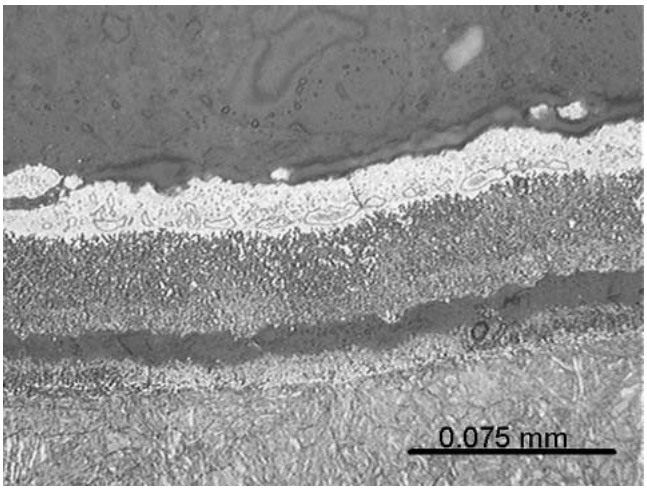

Fig. 11 Photomicrograph of the root area of the 3%Cr-Mo-V steel gear sample after nitriding at 538 °C for 354 h at 3.2 mbar in a mixture of 30% nitrogen and 70% hydrogen, etched with 2% nital. Note the very porous character of the compound zone and its delineation from the sample.

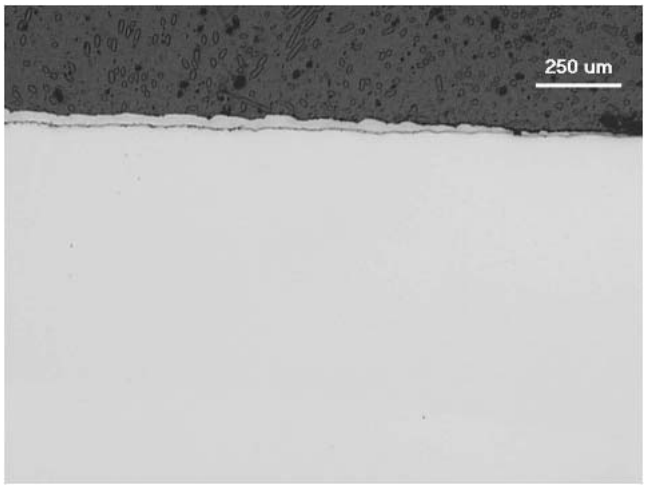

Fig. 12 Photomicrograph of the tooth flank of the 3%Cr-Mo-V steel gear sample between the pitch and the root after nitriding at 538 °C for 354 h at 3.2 mbar in a mixture of 30% nitrogen and 70% hydrogen, not etched. The left side of the picture is oriented toward the gear root. Note that the outer surface does not follow the straight line of the gear profile.

the pitch-flank area, although the degree of the differences varied depending on the processing pressure. There has to be another reason for the case-depth variation around the tooth in the gear sample other than a small temperature difference. The unetched structure of the tooth flank section is presented in Fig. 12. It can be seen that the contour of the gear flank toward the root (left side of the figure) deviates from a straight line and shows a built-up layer. It was very likely that this built-up layer had a strong effect on the structure and morphology of the compound zone. It was recently shown (Ref 26) that there could be a reduction in the nitriding kinetics of the diffusion zone depending upon the structure of the compound zone. Therefore, because the compound zone thickness and structures are not uniform in various locations of the gear sample, it

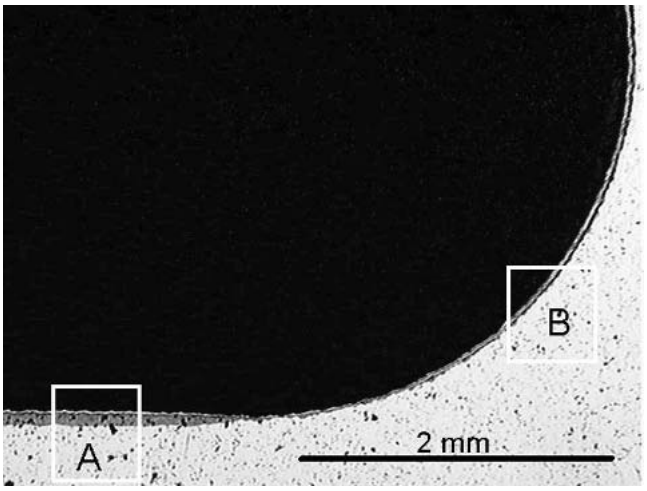

Fig. 13 Photomicrograph of the corner area of the 310 stainless steel slot sample nitrided at 580 °C for 15 h at 5.3 mbar in a mixture of 50% nitrogen and 50% hydrogen, etched with 2% nital. The sample was plated with nickel for better edge retention.

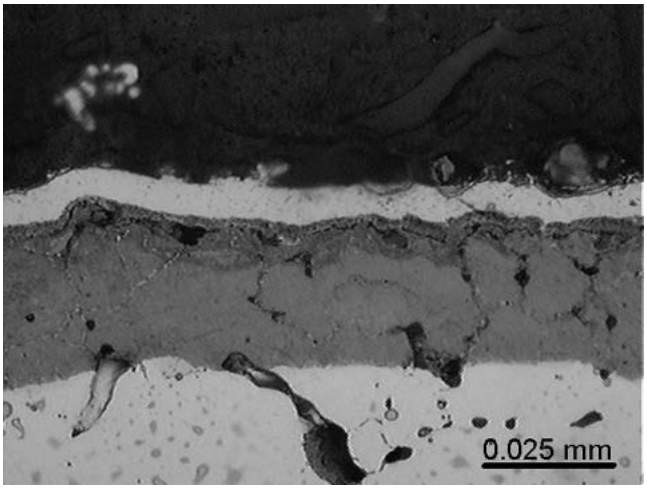

Fig. 14 Enlarged photomicrograph of flat area "A" of the 310 stainless steel slot sample shown in Fig. 13. Etched with 2% nital. Note the lightly etched outer nickel layer.

can be assumed that the resultant diffusion zone thickness in these locations will also not be uniform.

3.2 310 SS Slot

Photomicrographs of the 310 SS are presented in Fig. 13 to 15. The enlarged areas "A" and "B" in Fig. 14 and 15 show the case thickness to be nonuniform. The flat area of the sample slot had a uniform, 25 μm thick, nitrided layer as can be seen in Fig. 14. However, the picture in Fig. 15 shows that the nitrided layer has almost disappeared in the corner of the slot. In this area, there was a brittle and darker thin layer visible between the surface of the sample and the nickel-plating, as shown in Fig. 15. The location of this layer coincides with the inconsistent thickness of the nitrided layer in this area.

3.3 304 SS Flat

The case formed on the 304 stainless steel sample is shown in Fig. 16 to 19. The case in the corner of the sample was the

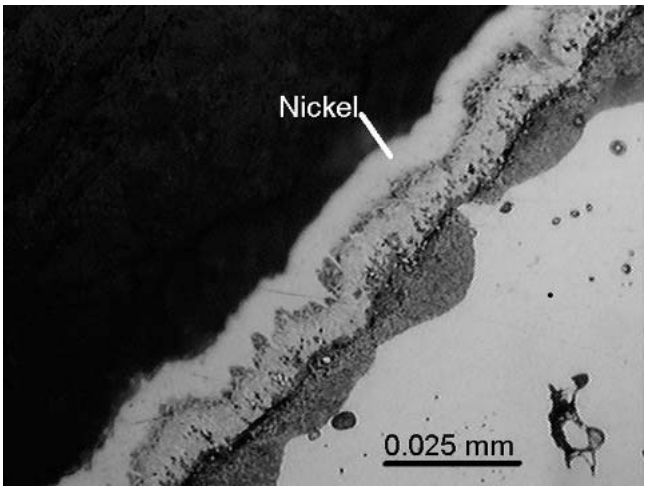

Fig. 15 Enlarged photomicrograph of flat area "B" of the 310 stainless steel slot sample shown in Fig. 13, etched with 2% nital. Note the lightly etched outer nickel layer and an intermediate layer underneath the top of the sample.

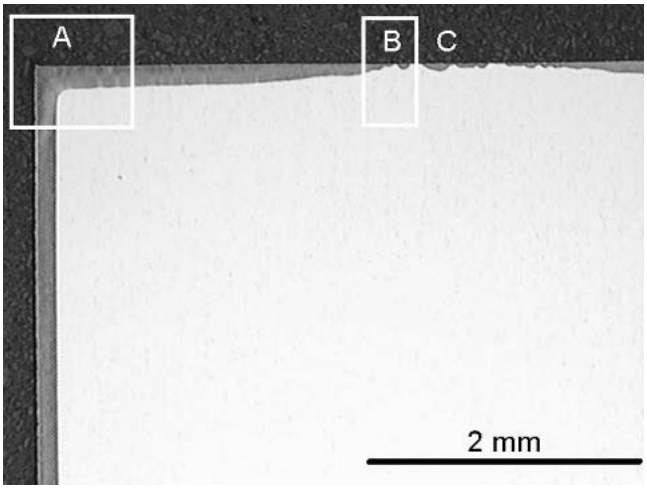

Fig. 16 Photomicrograph of the 304 stainless steel disc sample that was nitrided at 580 °C for 15 h at 3.00 mbar in a mixture of 50% nitrogen and 50% hydrogen, etched with 2% nital

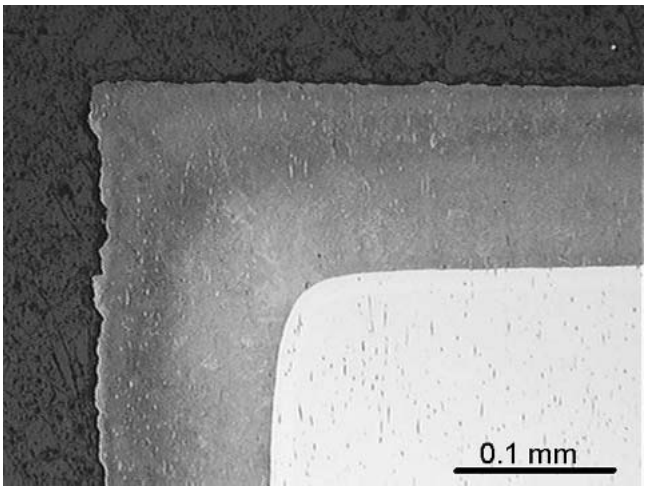

Fig. 17 Enlarged photomicrograph of the corner area "A" of the sample shown in Fig. 16, etched with 2% nital

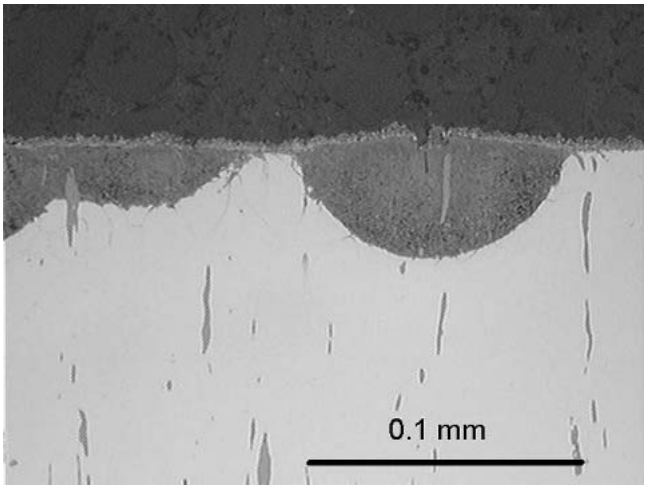

Fig. 18 Enlarged photomicrograph of the uneven case-depth area "B" of the sample shown in Fig. 17, etched with 2% nital. Note a porous, ~3 μm thick deposited layer on the sample surface.

thickest. The central section of the sample had a wavy, almost completely disappearing layer. Closer examination of the microstructure revealed the presence of a 2 to 3 μm thick (foreign) layer deposited at the top of the sample in the areas where the nitrided layer was not uniform.

3.4. Inconel 718 Fillet

The case formed on the Inconel 718 fillet sample is shown in Fig. 20 to 22. The case in the areas "A" and "B" was very uniform, although the surface of the sample was rough, with some evidence of a surface deposit. The area "C" adjacent to the fillet had only "spotty" nitrided areas as can be seen in Fig. 22. There was also a continuous deposited layer present on top of the sample in this area.

All of the results presented above demonstrate that plasma-nitrided layers may be, under certain processing conditions, very nonuniform. Although the mechanism of this common industrial problem is not completely clear, it seems that the main reasons for the formation of a nonuniform layer are related to sample/part geometry, as well as the nonuniform redeposition of sputtered atoms. Some of these problems can be corrected with proper pressure selection for plasma processing. As it is commonly known in the practice of plasma technology, there are two possible approaches. First, the glow seam follows the contour of the treated part, which occurs when a high processing pressure is used. In the second case, the glow seam is broad and foggy. This is the case when a lower processing pressure is used. However, there are many situations where the correction of the pressure may not completely solve all of the configuration problems. In situations like these, it is beneficial to use a reduced plasma power density to minimize the sputtering. This can be achieved with the hot wall technology or active screen plasma nitriding (Ref 27).

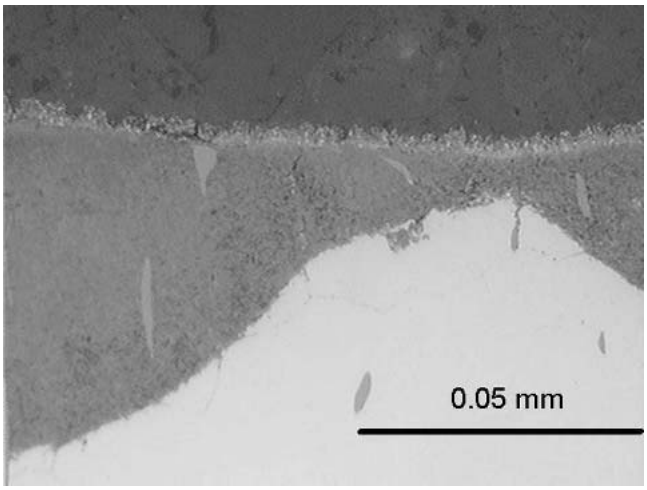

Fig. 19 Enlarged photomicrograph of the uneven case-depth area "C" of the sample shown in Fig. 16, etched with 2% nital

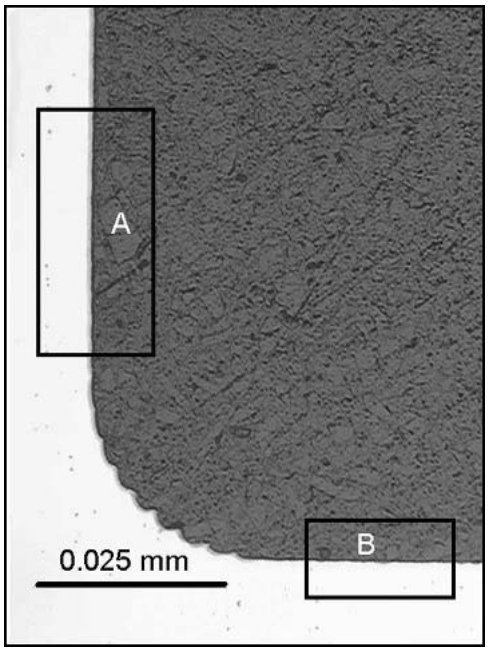

Fig. 20 Photomicrograph of the Inconel 718 fillet sample nitrided at 580 °C for 70 h at 8 mbar in a mixture of 70% nitrogen and 30% hydrogen, etched with 2% nital

4. Conclusions

Samples and parts of complex geometry may not achieve a uniform nitrided layer during plasma nitriding when processing is performed at an improper pressure for the configuration. Although the formation mechanism of these defective layers is not completely understood, there is strong evidence that the redistribution of the reactive sputtering products in those samples is the leading cause of the unevenness in the nitrided layer. The severity of this problem depends on the material processed. The nitrided case in the low-alloy 3%Cr-Mo-V steel sample was nonuniform but still very consistent, while the nitrided case in all of the stainless steel samples tested was locally disappearing from the surface. It can also be speculated

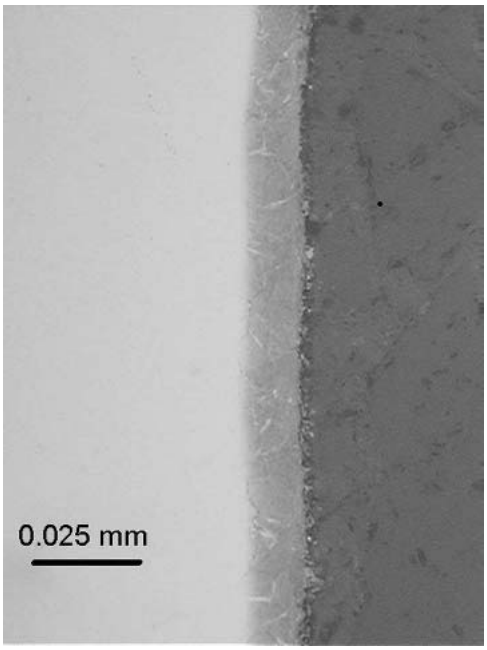

Fig. 21 Photomicrograph of the "A" area of the Inconel 718 fillet sample presented in Fig. 20, etched with 2% nital. Note the porous and noncontinuous layer present on the sample surface, and the uniform thickness of the nitrided layer.

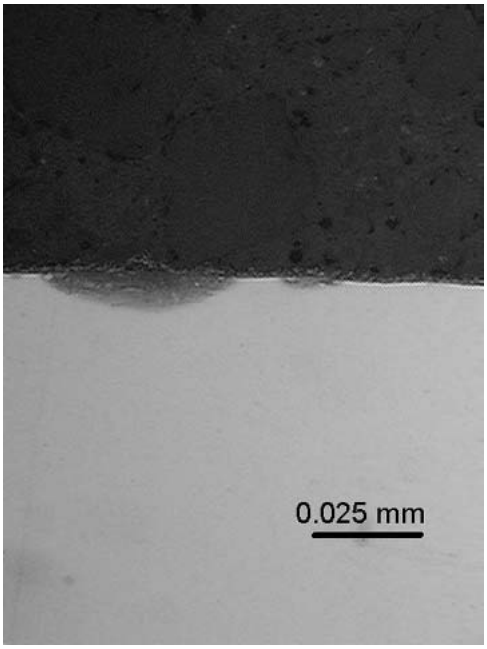

Fig. 22 Photomicrograph of the "C" area of the Inconel 718 fillet sample presented in Fig. 20, etched with 2% nital. Note a porous but continuous 1 to 2 μm thick deposited layer present on the sample surface and the uneven thickness of the nitrided layer.

that contamination of the nitriding system with oxygen or oxygen-bearing gases plays a more significant role in the formation of the vapor-deposited layer on the surface of the stainless steels, causing delay or inhibition of the nitriding reaction. However, this theory should be verified with a more extensive investigation of the surface structure and morphology of the samples.

References

1. J. Kölbel, *Tech. Bericht,* Institut der Gesellschaft zur Forderung der Glimmentladungsforschung, Cologne, 1966 (in German)
2. K. Keller, Schichtaufbau Glimnitrirter Eisenwekstoffe, *Härterei Technische Mitteilungen,* Vol 26, 1971, p 120-130 (in German)
3. B. Edenhofer, Physical and Metallurgical Aspects of Ion Nitriding, *Heat Treat. Metals,* Vol 23, 1974, p 59-67
4. T. Karpinski and E. Rolinski, Mechanismus des Ionnitrierens, *Proc. 8th National Conference on Heat Treatment,* Dom Techniky, Ed., CSVTS Bratislava, Slovakia, 1978, p 27-35 (in German)
5. A. Marciniak, Equilibrium and Non-Equilibrium Models of Layer Formation During Plasma and Gas Nitriding, *Surf. Eng.,* Vol 2, 1986, p 283-287
6. A. Wells and I. Le R. Strydom, Sputtering and Redeposition of Cathode Material During Plasma Nitriding, *Surf. Eng.,* Vol 2, 1986, p 283-267
7. A. Wells and I. Le R. Strydom, Influence of Sputtering and Redeposition on Compound Layer Growth During Plasma Nitriding, *Surf. Eng.,* Vol 4, 1988, p 55-59
8. T. Lampe, S. Eisenberg, and G. Laudien, Compound Layer Formation During Plasma Nitriding and Plasma Nitrocarburasing, *Surf. Eng.,* Vol 9 (No. 1), 1993, p 69-76
9. Y. Sun, N. Luo, and T. Bell, Three-Dimensional Characterisation of Plasma Nitrided Surface Topography, *Surf. Eng.,* Vol 10 (No. 4), 1994, p 279-286
10. H. Michel, T. Czerwiec, M. Gantois, D. Ablitzer, and A. Ricard, Progress in the Analysis of the Mechanism of Ion Nitriding, *Surf. Coat. Technol.,* Vol 72, 1995, p 103-111
11. Y. Sun and T. Bell, A Numerical Model of Plasma Nitriding of Low Alloy Steels, *Mater. Sci. Eng. A,* Vol 224, 1997, p 33-47
12. V.I. Dimitrov, J. D'Haen, G. Knuyt, C. Quaeyhaegens, and S.M. Stals, A Method for Determination of the Effective Diffusion Coefficient and Sputtering Rate During Plasma Diffusion Treatment, *Surf. Coat. Technol.,* Vol 99, 1998, p 234-241
13. E. Rolinski and G. Sharp, The Effect of Sputtering on Kinetics of Compound Zone Formation in the Plasma Nitriding of 3% Cr-Mo-V Steel, *J. Mater. Eng. Perf.,* Vol 10 (No. 4), 2001, p 444-448
14. J. P. Leburne, H. Michel, and M. Gantois, Nitruration par Bombardement Ionique des Aciers Inoxydables 18-8, *Mém. Sci. Rev. Métall.,* Vol 69, 1972, p 727-749 (in French)
15. V.J. Coppola, Gas Nitriding of Stainless Steel, *Source Book on Nitriding,* ASM, 1977, p 219-220
16. "Ion Nitriding," GE Aircraft Engines Specification No. P11TF10, (No. 53) 1996, p 1-13
17. C. Ruset, V. Stoica, S. Janosi, Z. Koloszvary, A. Bloyce, and T. Bell, The Influence of Oxygen Contamination on Plasma Nitrided and Nitrocarburized Layers, *Proc. 11th Congress of the International Federation for Heat Treatment and Surface Engineering,* Ed. Associazione Italiana di Metallurgia, Milano, Italy, Vol 1, 1998, p 271-279
18. G. Tibbets, Role of Nitrogen Atoms in Ion-Nitriding, *J. Appl. Phys.,* Vol 45 (No. 11), 1974, p 5072-5073
19. G. Nayal, D.B. Lewis, M. Lembke, W. D. Münz, and J.E. Cockrem, Influence of Sample Geometry on the Effect of Pulse Plasma Nitriding of M2 Steel, *Surf. Coat. Technol.,* Vol 111, 1999, p 148-157
20. C. Alves, E.F. da Silva, and A.E. Martinelli, Effect of Work Piece Geometry on the Uniformity of Nitrided Layers, *Surf. Coat. Technol.,* Vol 139 (No. 1), 2001, p 1-5
21. Y. Sun, T. Bell, Z. Kolosvary, and J. Flis, The Response of Austenitic Stainless Steels to Low-temperature Plasma Nitriding, *Heat Treat. Metals,* Vol 45 (No. 1), 1999, p 9-16
22. Williamson Corporation, *Non-Contact Temperature Measurement, Monitoring and Control,* Williamson Corporation, Concord, MA, 1994
23. B. Reinhold, B. Larish, and H.-J. Spies, Control of Plasma Nitriding Using Oxygen Probes, *Surf. Coat. Technol.,* Vol 142-144, 2001, p 365-370
24. S. Parascandola, W. Möller, and D.L. Williamson, Successful Nitriding of Austenitic Stainless Steel: The Diffusion Mechanism of Nitrogen and the Role of the Surface Oxide Layer, *Proc. Stainless Steel 2000,* Maney Publishing for The Institute of Materials, London, 2001, p 201-214
25. E. Rolinski, F. LeClaire, D. Clubine, G. Sharp, D. Boyer, and R. Notman, Kinetic of Plasma Nitriding and Renitriding of 3% Cr-Mo-V Steel, *J. Mater. Eng. Perf.,* Vol 9 (No. 4), 2000, p 457-462
26. J. Ratajski, J. Tacikowski, and T. Suszko, "Role of the Layer of Iron (carbo) Nitrides in the Kinetics of Diffusion Layer Growth on Alloy Steels," Paper presented at the International Conference on Nitriding (Warsaw, Poland), September 2003
27. J. Georges and D. Cleugh, Active Screen Plasma Nitriding, *Proc. Stainless Steel 2000,* T. Bell and K. Akamatsu, Ed., Maney Publishing for The Institute of Materials, London, 2001, p 377-388